Supporting Information

NIR-Responsive Polypeptide Nanocomposite Generates NO Gas, Mild Photothermia and Chemotherapy to Reverse Multidrug Resistant Cancer

Yue Ding, Chang Du, Jiwen Qian, Chang-Ming Dong*

School of Chemistry and Chemical Engineering, Shanghai Key Laboratory of Electrical Insulation and Thermal Aging, Shanghai Jiao Tong University, Shanghai 200240, P. R. China

Experimental Section

Materials. Dimethylformamide (DMF, 99.5%) was distilled from calcium hydride under reduced pressure and stored over 4Å molecular sieves. Dopamine hydrochloride (98%, Aldrich), tris(hydroxymethyl) methyl aminomethane (Tris, >99.9%, Aldrich) and tert-butyl nitrite (TBN, 95%, J&K) were used as received. Doxorubicin (DOX) hydrochloride was purchased from Beijing Huafeng United Technology Corp. and used as received. According to our previous publications,[1,2] poly(ethylene glycol)$_{45}$-b-poly(L-cysteine)$_{20}$ (PC, yield 87.4wt%) was synthesized by amino-terminated poly(ethylene glycol)$_{45}$ (PEO, M_n = 2000) initiated ring-opening polymerization of S-(o-nitrobenzyl)-L-cysteine N-carboxyanhydride, followed by the full photocleavage of o-nitrobenzyl groups. ^{1}H NMR of PC (DMSO-d_6): δ (ppm) = 5.35-4.25 (m, SHCH$_2$C*H*, 20H), 3.78-3.57 (m, O(C*H*$_2$C*H*$_2$O)$_{45}$, 180H), 3.48 (s, –O*CH*$_3$, 3H), 2.92-2.85 (m, SH*CH*$_2$CH, 40H).

Anti-P-gp antibody (ab129450, Abcam), Dulbecco's modified eagle medium (DMEM, PAA Laboratories), fetal bovine serum (FBS, PAA Laboratories), hoechst33342 (Ultra Pure, Aldrich), and methylthiazolyldiphenyl-tetrazolium bromide (MTT, Ultra Pure, Aldrich) were used as received. L929 (a mouse fibroblastic cell line), MCF-7 (a human breast carcinoma cell line) and MCF-7/ADR (a human breast MDR cancer cell line) were received from Shanghai Institute of Biochemistry and Cell Biology.

Methods. Fourier transform infrared (FT-IR) spectroscopy was recorded on a Perkin Elmer Spectrum 100 spectrometer. ^{1}H NMR (400 MHz) spectra was recorded on a Varian Mercury-400 spectrometer. X-ray photoelectron spectroscopy (XPS) was conducted on a VG ESCALAB MKII spectrometer and analyzed by the XPS PEAK software (Version 4.1). Dynamic light scattering (DLS) was used to determine the average hydrodynamic diameter and polydispersity index (PDI) of nanoparticles on a Malvern ZS90 instrument. Transmission electron microscopy (TEM, JEM-2010, JEOL) and field emission transmission electron microscopy (FE-TEM, TALOS F200X, FEI) were performed without negative staining at 200 kV accelerating voltage, during which a little nanoparticle solution was dropped on the Formvar-carbon film-coated copper grids and allowed to dry in air; the energy-dispersive X-ray (EDX) spectroscopy was obtained simultaneously to analyze the elemental composition. The UV-Vis-NIR spectroscopy was recorded on a Perkin-Elmer Lambda 750S spectrometer. The fluorescent spectroscopy was recorded on a Perkin-Elmer LS-50B spectrometer. Super-resolution multiphoton confocal laser

scanning microscopy (CLSM) was performed on a Leica TCS SP8 STED 3X instrument. All the 808 nm NIR irradiations were carried out by using a continuous wave diode laser (Shanghai SFOLT Corp., FC-960-6000-MM) with tunable power (0–1650 mW), during which process the spot size was tuned by a fiber collimator connected by a fiber optic patch cable (FC/PC/200UM/1M).

Preparation of the polypeptide block copolymer PNOC. The polypeptide block copolymer with pendant S-nitroso (SNO) groups ($PNOC_n$, the subscript denotes the SNO number) was prepared from the PC with pendant SH groups (**Scheme S1**). Briefly, PC (120.0 mg, 29.55 mmol) was dissolved in 2 mL DMF, and then 80 μL TBN was added. The resulting solution was stirred at room temperature for 24 h in dark and then precipitated dropwise into a large excess of diethyl ether (16 mL). The yellow precipitate was centrifuged, rapidly dried in vacuum, and finally stored in dark to give 126.6 mg of $PNOC_{20}$ (yield: 92.3%). ^{1}H NMR (DMSO-d_6) of $PNOC_{20}$: δ (ppm) = 5.32-4.22 (m, $SNOCH_2CH$, 20H), 3.78-3.57 (m, $O(CH_2CH_2O)_{45}$, 180H), 3.48 (s, $–OCH_3$, 3H), 2.87-2.81 (m, $SNOCH2CH$, 40H).

Fabrication of the PNOC-PDA nanocomposite. The PNOC-PDA nanocomposite was simply fabricated by two steps. First, the PNOC in DMF solution (5 mL, 2 mg/mL) was gradually added with 0.5 mL distilled water under vigorous stirring overnight, and then dialyzed against distilled water (MWCO: 3500 Da) for 24 h to produce the PNOC micelle solution. In the next step, 1 mL PNOC micelle solution was directly added with 1 mL dopamine hydrochloride (4.0 mg/mL) in Tris buffer (10 mg/mL) and then stirred vigorously for 4 h at room temperature. The resulting

suspension was centrifuged at 17000 rpm for 30 min, and then the precipitate was washed for three times with 10 mL distilled water. The precipitate was dispersed again in 3.4 mL distilled water to give the nanocomposite solution (i.e. PNOC-PDA, 1.0 mg/mL). Analyzed by XPS, the PDA component in $PNOC_{20}$-PDA can be calculated by the equation: PDA (wt%) = 100% − S% ($PNOC_{20}$-PDA)/S% ($PNOC_{20}$) = 100% − 4.09%/16.9% = 75.8 wt%, where S% ($PNOC_{20}$-PDA) is directly obtained by XPS and S% ($PNOC_{20}$) is the theoretical composition of sulfur in $PNOC_{20}$.

Preparation and In vitro stimuli-responsive drug release of DOX-loaded nanocomposite PNOC-PDA/DOX. Generally, 3 mL DOX·HCl aqueous solution (1 mg/mL) was added into 2 mL PNOC-PDA (1.0 mg/mL) under vigorous stirring at room temperature. After 24 h incubation, PNOC-PDA/DOX was collected via centrifugation at 17000 rpm for 30 min, and then washed with 10 mL distilled water for three times. The precipitate was dispersed again in 3.4 mL distilled water or PBS (10 mM, pH 7.4) to produce the DOX-loaded PNOC-PDA nanocomposite (i.e. PNOC-PDA/DOX, 1.0 mg/mL).

As for pH triggered release, the PNOC-PDA/DOX in PBS (2 mL, 10 mM, pH 7.4) was transferred into a dialysis bag (MWCO = 3500 Da), and then incubated in 10 mL PBS (pH = 5.0 and 7.4) with a shaking rate of 150 rpm at 37 °C. As for the NIR-triggered release, the above samples were vertically irradiated at prescribed times and then put into 10 mL PBS at 37 °C. Then 10 mL dialysis solution was taken out at predetermined times and same volume of fresh PBS was added back. The released DOX amount was measured at 490 nm by UV-Vis spectroscopy. All release

experiments were carried out in duplicate.

In vitro NO release and photothermal property of PNOC-PDA. The NO release in aqueous solution was quantitatively measured by a typical Griess assay.[3] Briefly, 200 μL PNOC-PDA (1.0 mg/mL) in a 96-well plate was vertically irradiated (808 nm, 1 W/cm^2, 10 min) every half hour, and the released NO amount was determined by using a microplate reader (λ = 540 nm). Meanwhile, 200 μL PNOC-PDA solutions with different concentrations were irradiated for recording the temperature change curves and the repeated heating-cooling cycles (i.e., 10 min NIR irradiation and 10 min naturally cooling) by a digital thermometer.

In vitro cell studies. L929, MCF-7 and MCF-7/ADR cell lines were cultured at 37 °C in Dulbecco's Modified Eagle's Medium (DMEM) supplemented with 10% fetal bovine serum (FBS), 100 IU/mL penicillin, and 100 μg/mL streptomycin under a humidified atmosphere of 5 % CO_2. Briefly, 200 μL of cells suspension in DMEM was added to each well in a 96-well plate (1×10^4 cells/well) and cultured for 24 h. 200 μL of the nanocomposites PNOC-PDA or PNOC-PDA/DOX or the counterparts (PC-PDA or PC-PDA/DOX) with different concentrations were added into wells and incubated with cells for 48 h. After that, the standard MTT assay was carried out to determine the cell viability by a Microplate Reader (Elx800, BioTek Company).

To evaluate PTT (PC-PDA), PTT-NO (PNOC-PDA), PTT-CT (PC-PDA/DOX), and PTT-NO-CT (PNOC-PDA/DOX), a series of the nanocomposite solution with gradient concentration were added separately into a 96-well plate and incubated for 4 h at 37 °C with/without the NIR irradiation (808 nm, 1 W/cm^2, 10 min). The cells

were further incubated for 48 h and then assessed by MTT. Half maximal inhibitory concentration (IC_{50}) was calculated by GraphPad Prism 6 software using five samples. As for single CT and the combination CT, the IC_{50} values were calculated on the basis of DOX concentration; those for PTT-NO and the combination one were calculated by pure PDA in PNOC-PDA or PNOC-PDA/DOX; those for single PTT and the combination PTT was obtained by calculating pure PDA in PC-PDA or PC-PDA/DOX. The combination index (CI) was calculated by the following equation: CI = [IC_{50} (combination CT)/IC_{50} (CT)] + [IC_{50} (combination PTT-NO)/IC_{50} (PTT-NO)].[4] All cell viabilities were tested in six replicates.

Cell internalization. Using MCF-7/ADR as the model cell line, the cell internalization process of free DOX or PNOC-PDA/DOX was monitored by flow cytometry (BD Accuri C6, US BD Corporation) and inverted fluorescence microscopy (LeicaDMI6000 B). Briefly, MCF-7/ADR was incubated in 6-well tissue culture plate (5.0×10^5cells per well) for 24 h. The same drug concentration of free DOX or PNOC-PDA/DOX (10 μg/mL DOX equiv) was added to per well for predetermined time at 37 ^oC with or without the NIR irradiation. The cells were rinsed with PBS, disposed with trypsin, and then the collected data for 1.0×10^4 gated events were analyzed by FlowJo software. After similar treatment, MCF-7/ADR was fixed with 4% formaldehyde for 30 min at room temperature, washed with PBS, stained by Hoechst33342 for 15 min, and finally observed by CLSM. Data were analyzed using ImageJ software.

Measurement of P-gp expression. The P-gp expression was detected by western blot

analysis and flow cytometry. MCF-7/ADR was incubated in 6-well plate for 24 h and then incubated with PBS, DOX, PC-PDA/DOX, PNOC-PDA/DOX, and PC-PDA/DOX and PNOC-PDA/DOX (10 μg/mL DOX equiv) plus NIR irradiation for another 24 h. After stained by anti-Pgp antibody for 20 min, MCF-7/ADR was digested with trypsin and the collected data for 1.0×10^4 gated events were analyzed by FlowJo software. After similar treatment, the MCF-7/ADR cells were centrifuged at 1000 rpm for 10 min, washed with cold PBS for three times, and suspended in RIPA lysis buffer. The lysates were centrifuged and the supernatant was collected. Protein concentration was determined using bicinchoninic acid (BCA) protein assay (Thermo Fisher Scientific). The total protein was determined using the BCA protein assay reagent, and each sample was resolved via sodium dodecyl sulfate polyacrylamide gel electrophoresis and then transferred to a polyvinylidene fluoride membrane. After incubation in 2% BSA for 60 min, the membrane was incubated with anti-P-gp antibody at 4 °C overnight. Finally, the membrane was incubated with secondary antibody for 30 min at room temperature, washed with TBST for three times and visualized using ChemiDoc MP detection system (Bio-Rad).

Animals. 5-week-old male Balb/c nude mice (~20 g) and Sprague−Dawley (SD) rats (~200 g) were purchased from Chinese Academy of Sciences (Shanghai, China). The animal experiments were performed in accordance with the guidelines for the care and use of laboratory animals and approved by the Animal Ethics Committee of Shanghai Jiao Tong University.

Pharmacokinetics. The SD rats were randomly divided into two groups (n = 4) and

each mouse was injected via tail vein with 8 mg/kg free DOX or PNOC-PDA/DOX equiv. The blood samples (0.3 mL) were obtained via eye puncture at selected time intervals (i.e., 0.25, 0.5, 1, 2, 4, 6, 8, 12, 14 and 24 h). Plasma samples were harvested by immediate centrifugation (10 min, 3000 rpm), frozen at − 20 °C, and then the DOX in blood serum was analyzed by fluorescence spectroscopy. The pharmacokinetic parameters were calculated by using OriginPro 9.

In vivo multiple imagings and biodistributions. The MCF-7/ADR tumor-bearing nude mice with a tumor volume (~300 mm^3) were intravenously injected via tail vein with 200 μL of PNOC-PDA/DOX (2 mg/mL) or free DOX (5.3 mg/kg). In vivo fluorescent imaging was monitored at 1, 2, 4, 6, 8, 10, 12 ,14 and 24 h post-injection using a Kodak multimode imaging system (DOX: λex = 530 nm, λem = 600 nm). For ex vivo distributions, after the mice were sacrificed by cervical vertebra dislocation at 2 h, 6 h and 10 h post-injection (n = 3), all tumor and major organs were collected, washed with saline, and then imaged. The DOX amount in all tissues were respectively extracted with 1.2 mL HCl-IPA, measured by fluorescence spectroscopy, and given as the percentage injected dose per gram tissue (% ID/g).

As for in vivo hyperthermia and imaging, the mice (n = 4) were intravenously injected with 200 μL (2 mg/mL) of PNOC-PDA or PNOC-PDA/DOX or the control PBS, and then irradiated by the NIR laser (808 nm, 1 W/cm^2, 10 min) at 10 h post-injection. The thermographic image and the tumor temperature were recorded by an infrared thermal camera (AXT100, Ann Arbor Sensor Systems).

After 200 μL (2 mg/mL) of PNOC-PDA/DOX or the control PNOC-PDA was

intravenously injected into the mice (n = 3), the photoacoustic (PA) imaging was acquired at 1, 2, 4, 6, 8, 10, 12, 14 and 24 h post-injection using a commercial Endra Nexus 128 PA tomography system (Endra Inc., Ann Arbor, Michigan) equipped with a tunable nanosecond pulsed laser (808 nm, 7 ns pulse, 7 mJ/pulse, 2 Hz pulse repetition frequency) and a 128 unfocused ultrasound transducer with a 5 MHz center frequency. The PBS alone was used to eliminate the background signal for obtaining the PA signal of PNOC-PDA and/or PNOC-PDA/DOX.

In vivo antitumor activity. The MCF-7/ADR tumor-bearing mice with a tumor volume (60–80 mm^3) were randomly divided into seven groups (n = 4). All the mice were intravenously injected once on day 0 with 5 mg/kg DOX or nanoparticles (PNOC-PDA or PNOC-PDA/DOX, 200 μL, 2 mg/mL) or PBS. As for the PNOC-PDA+NIR and PNOC-PDA/DOX+NIR groups, the tumor sites were irradiated by the NIR laser (808 nm, 1 W/cm^2, 10 min) at 10 h post-injection. Tumor volume (V) is calculated according to the following equation: V (mm^3) = 1/2 × length (mm) × width (mm) × width (mm). The tumor inhibitory rates (TIR) of various treatments are calculated by the equation: TIR (%) = 100 × (mean tumor volume of the PBS group – mean tumor volume of others)/(mean tumor volume of the PBS group). When the tumor volume of the PBS group reached ~1500 mm^3 on day 30, one mouse from each group was sacrificed for comparative studies. Finally the tumors as well as major organs (heart, liver, spleens, lung and kidneys) were dissected, washed with saline, weighted, photographed, and fixed with 4% formaldehyde for H&E staining, TUNEL, and PCNA assays. All the mice were euthanized if the tumor volume was larger than

1500 mm^3 or the body weight loss was greater than 15%. Statistical analyses were performed using GraphPad Prism software 5.0 and data were given as mean ± S.D.

Statistical analysis. The two-way analysis of variance and the t-test were used to determine statistical significance. A probability (P) value < 0.01 was considered significant, and P < 0.001 was highly significant. All computations were made by employing Microsoft Excel 2007.

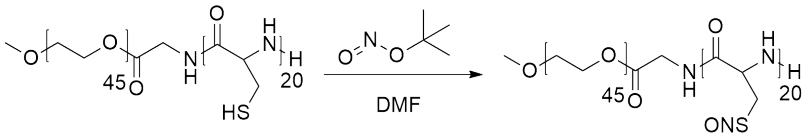

Scheme S1. Synthesis of $PNOC_{20}$.

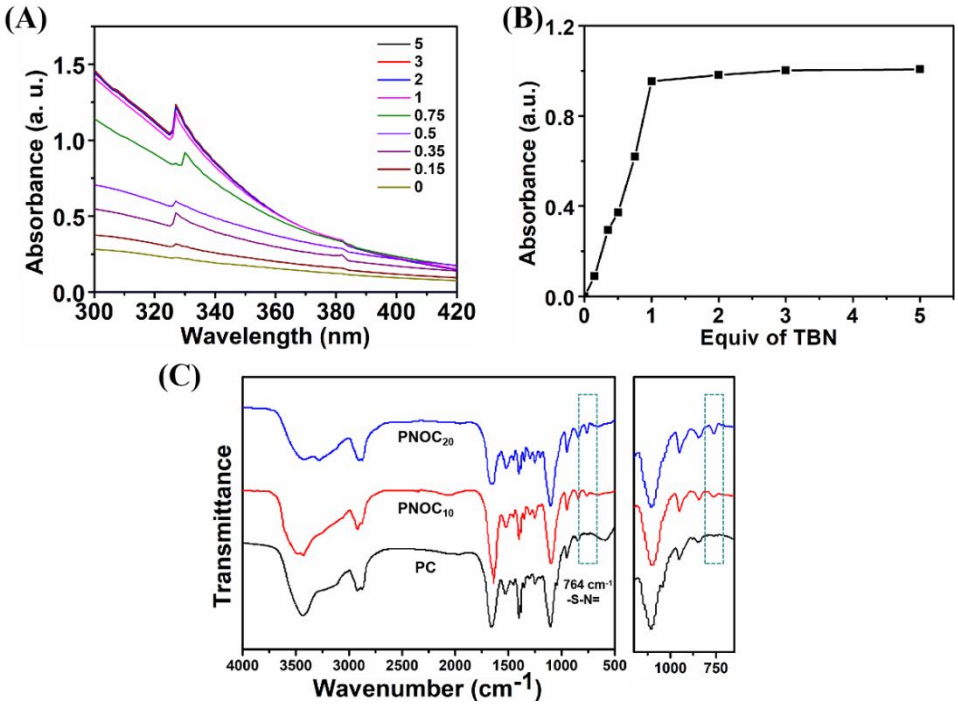

Figure S1. (A) UV-Vis-NIR spectra of PNOC in DMF with equiv of TBN to -SH; (B) dependence of absorbance at 327 nm of PNOC in DMF with molar ratio of TBN to -SH; (C) FT-IR for PC and PNOC, PNOC.

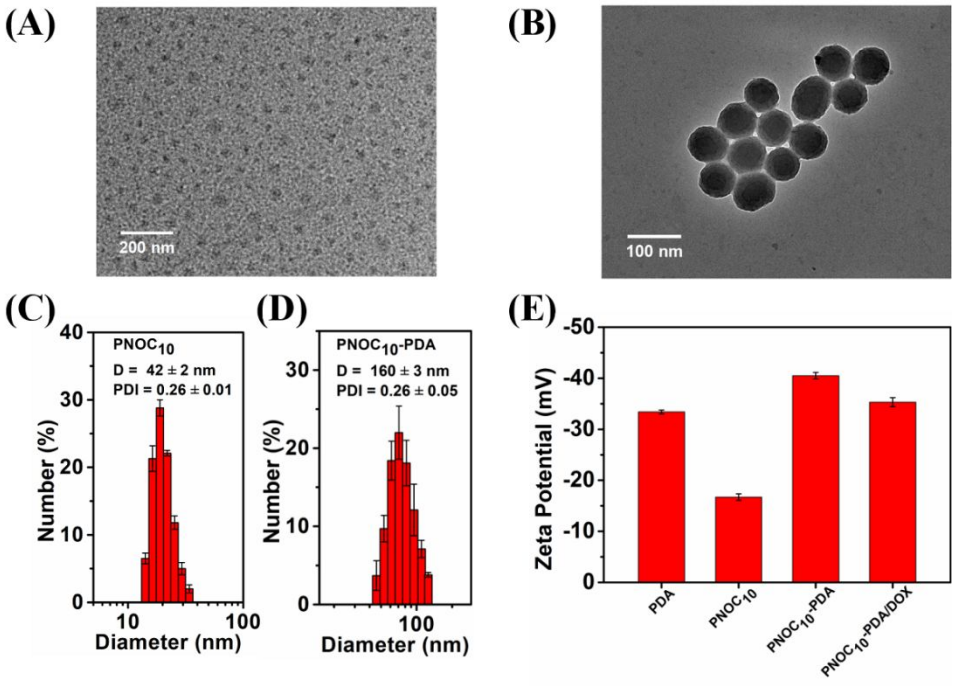

Figure S2. TEM images and DLS data of $PNOC_{10}$ (A, C) and $PNOC_{10}$-PDA (B, D); (F) Zeta potential for PDA, $PNOC_{10}$, $PNOC_{10}$-PDA and $PNOC_{10}$-PDA/DOX.

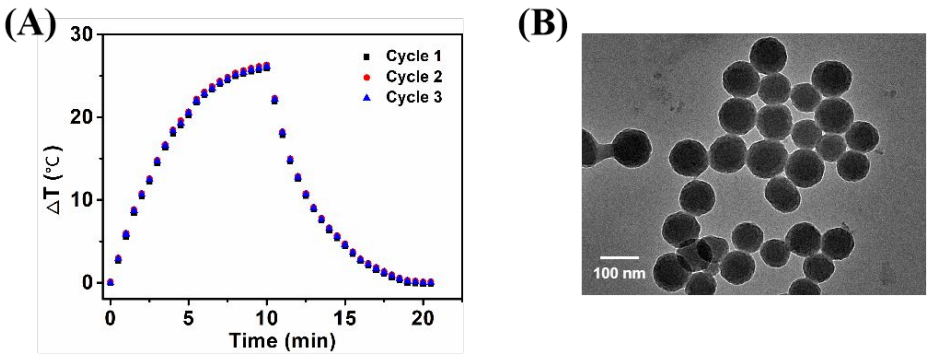

Figure S3. (A) The magnitude of temperature elevation (ΔT) of the $PNOC_{10}$-PDA solution during laser on/off cycles; (B) the TEM image of $PNOC_{20}$-PDA after 10 min NIR irradiation.

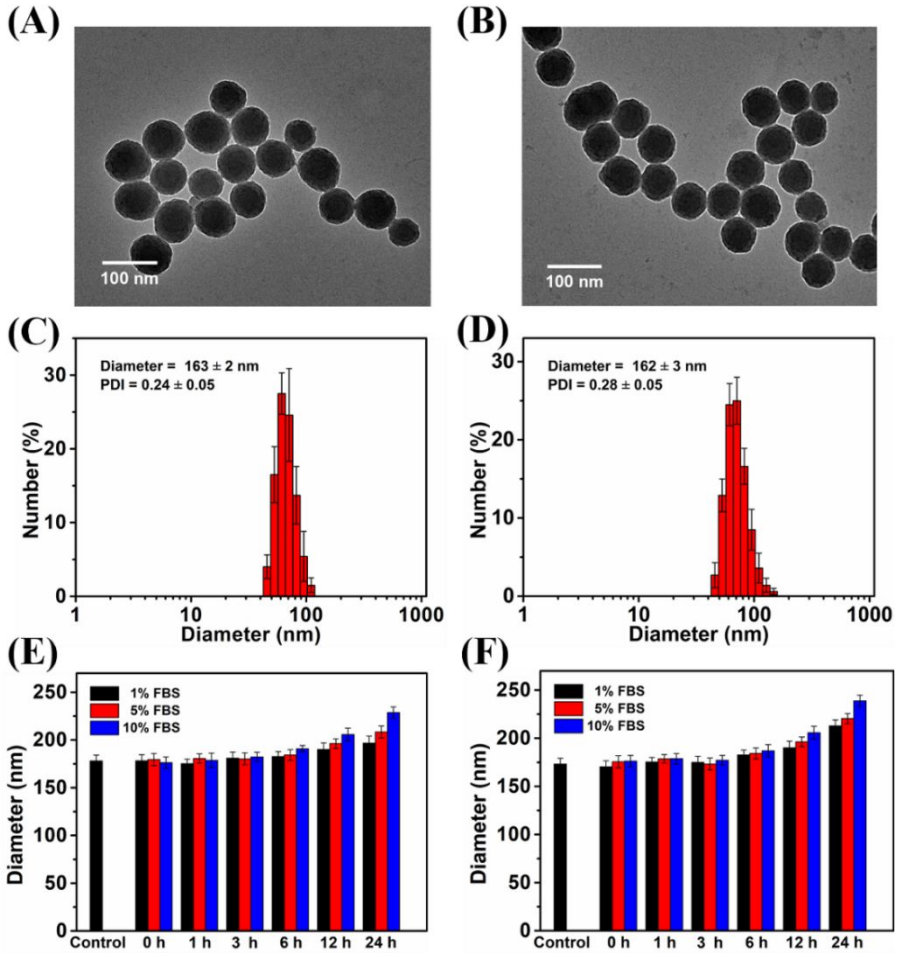

Figure S4. TEM images and DLS data of $PNOC_{10}$-PDA/DOX (A, C) and $PNOC_{20}$-PDA/DOX (B, D); the dependence of the DOX-loaded nanocomposite size on incubation time in FBS at 37 °C for $PNOC_{10}$-PDA/DOX (E) and $PNOC_{20}$-PDA/DOX (F).

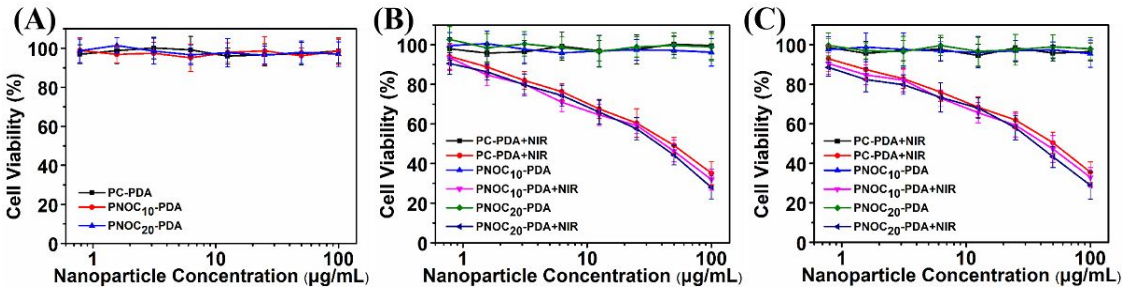

Figure S5. Cytotoxicity of PC-PDA, $PNOC_{10}$-PDA and $PNOC_{20}$-PDA incubated with L929 (A), MCF-7 (B) and MCF-7/ADR (C) with/without the NIR irradiation.

We applied flow cytometry and CLSM to study the intracellular DOX transport and

the MDR-reversing ability of PNOC-PDA/DOX with/without NIR irradiation (**Fig. S6-7**). By measuring the DOX fluorescence using flow cytometry, the intracellular uptake of free DOX for MCF-7/ADR was significantly inhibited about 245% at 4 h compared to that of MCF-7, showing a severe MDR of MCF-7/ADR to DOX; by CLSM, this was observed with a much weaker DOX fluorescence in MCF-7/ADR than that in MCF-7 incubated with DOX for 4 h. However, for MCF-7 and MCF-7/ADR, both $PNOC_{10}$-PDA/DOX and $PNOC_{20}$-PDA/DOX greatly enhanced intracellular DOX uptake for about 51–61% and 239–306% compared to free DOX, which was observed by the brighter DOX fluorescence in those cells with pink one in main nuclei (i.e., the merged color of red DOX and blue Hoechst3342). This is reasonable as PNOC-PDA/DOX with a diameter of < 200 nm can efficiently transport DOX into cells via an energy-mediated endocytosis process compared to a passive diffusion of free DOX, thus increasing intracellular DOX accumulation enormously. Moreover, upon NIR irradiation, the DOX fluorescence intensity at 4 h increased about 64–69% and 95–108% for both MCF-7 and MCF-7/ADR treated with PNOC-PDA/DOX than those without NIR irradiation, which was vividly observed by the brightest DOX fluorescence in those cells with stronger pink one in nuclei. This is because the NIR irradiation can enhance the membrane permeation and endolysosomes disruption, thus inducing a higher cellular internalization and subcellular trafficking. Notably, comparing $PNOC_{20}$-PDA/DOX+NIR to $PNOC_{10}$-PDA/DOX+NIR, the DOX fluorescence intensity at 4 h increased about 130% for MCF-7/ADR, suggesting more NO release effectively reversed the MDR of

MCF-7/ADR to DOX, as also evidenced by CLSM. In all, these results convincingly demonstrated that the triple therapies of PT-NO-CT based on PNOC-PDA/DOX+NIR could effectively transport much more DOX into cytoplasm until nucleus of the DOX-resistant MCF-7/ADR because of the NO-mediated MDR-reversal and the hyperthermia-enhanced membrane permeability and internalization.

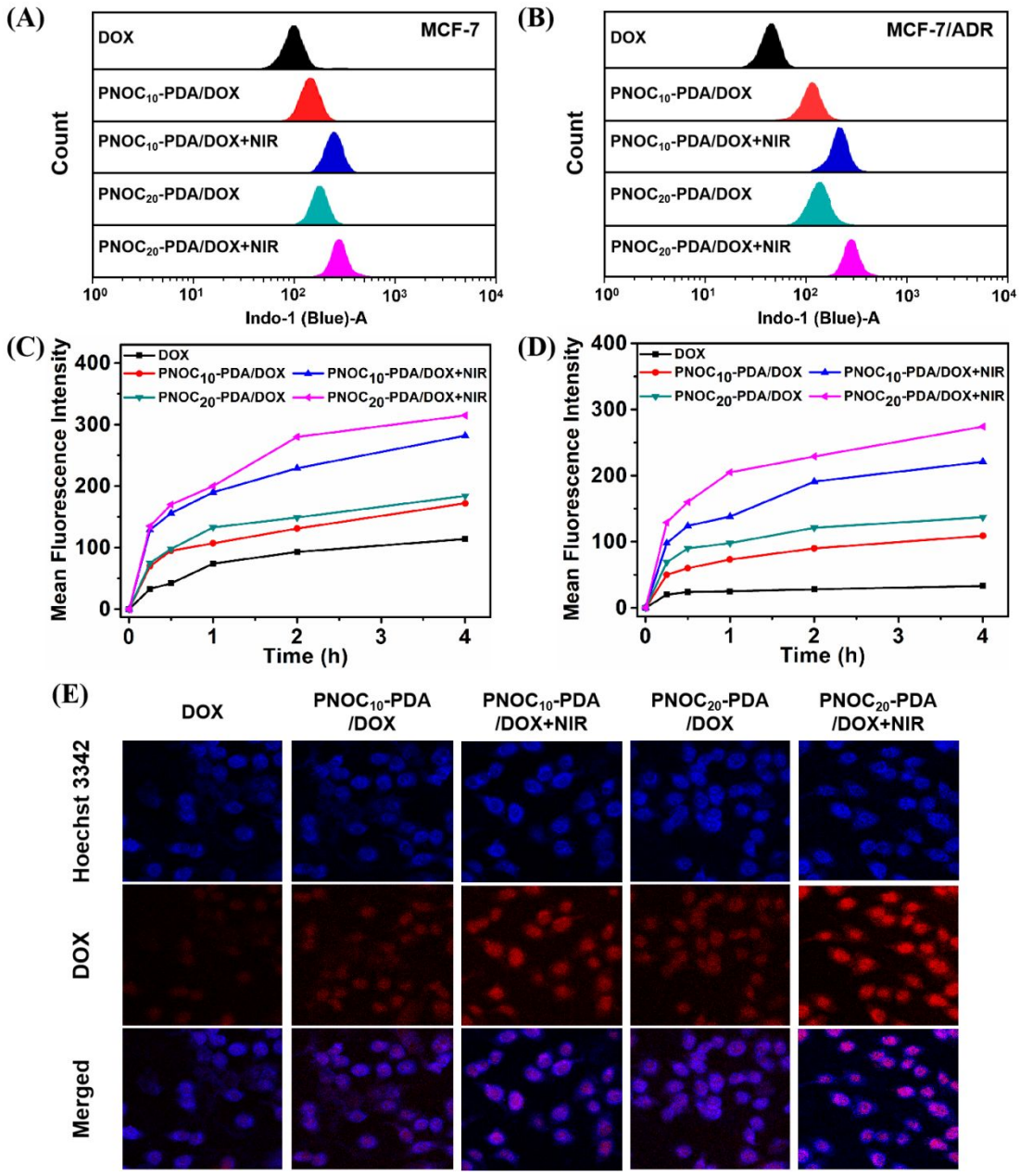

Figure S6. Flow cytometry histograms and the time-dependent fluorescence intensity of MCF-7 (A, C) and MCF-7/ADR (B, D) incubated with DOX and

PNOC-PDA/DOX at different conditions; (E) CLSM images of MCF-7/ADR incubated with DOX and PNOC-PDA/DOX for 4 h at different conditions.

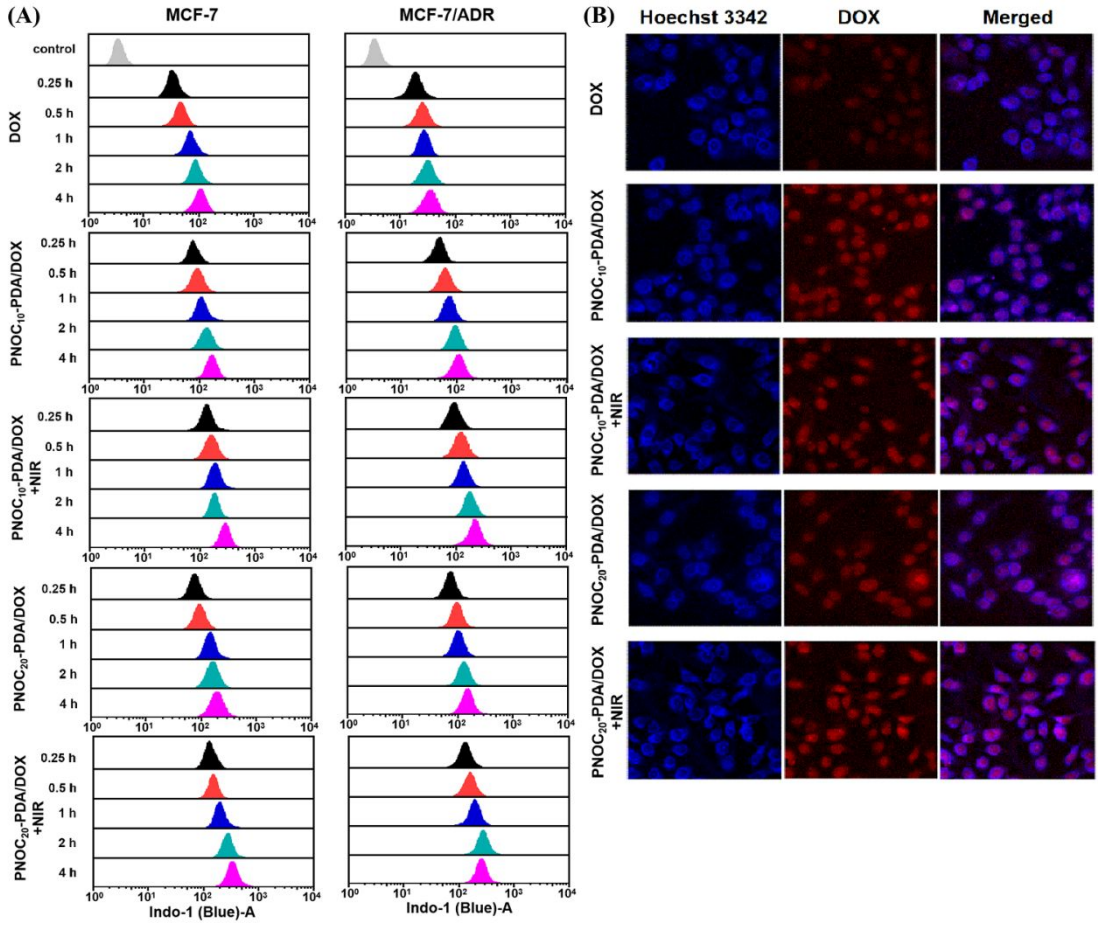

Figure S7. (A) Flow cytometry histograms of MCF-7 and MCF-7/ADR incubated with DOX, $PNOC_{10}$-PDA/DOX and $PNOC_{20}$-PDA/DOX for different times and at different conditions; (B) CLSM images of MCF-7 incubated with DOX, $PNOC_{10}$-PDA/DOX and $PNOC_{20}$-PDA/DOX for 4 h at different conditions.

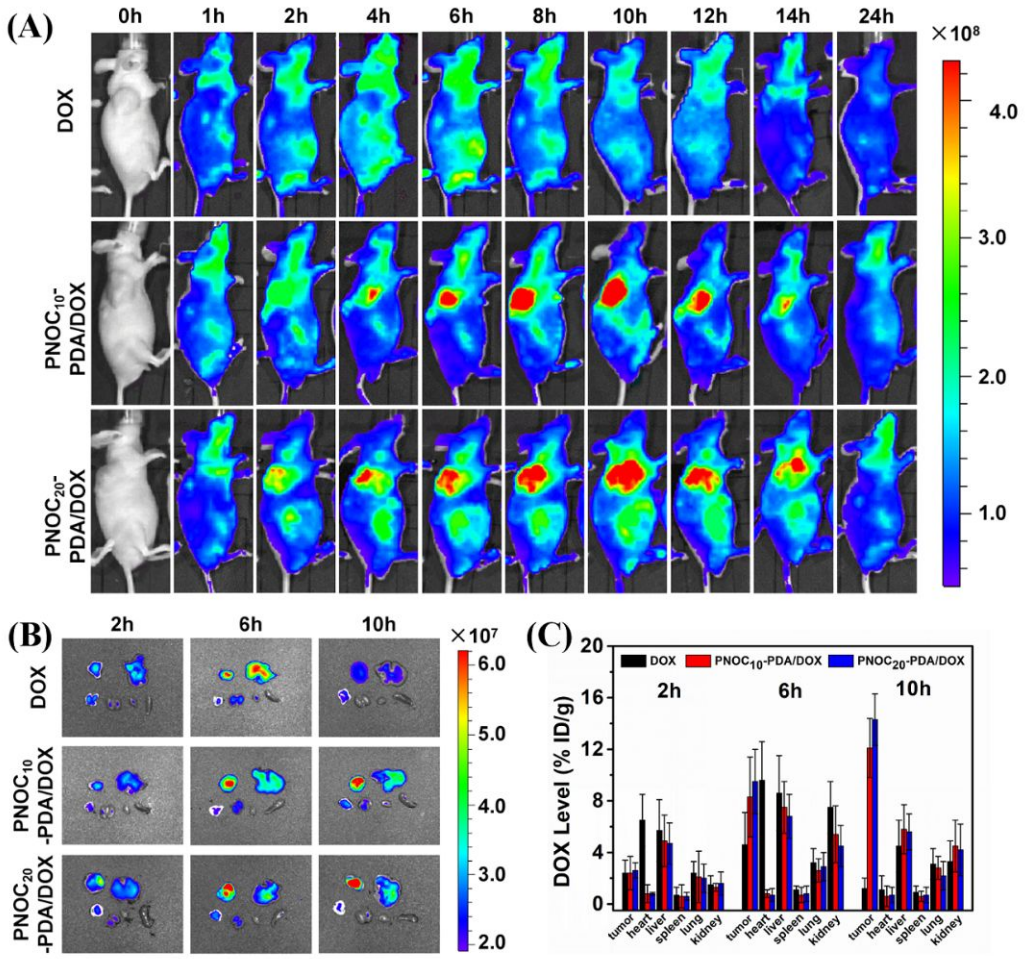

Figure S8. (A) In vivo fluorescent imaging of the tumor-bearing nude mice after intravenous injection of DOX and PNOC-PDA/DOX at different times; (B) Ex vivo imaging of the major organs and the tumor; (C) biodistributions of DOX in different organs and tumor at a DOX dosage of 5.0 mg/kg (n = 3).

Following intravenous injections in SD mice and collecting blood samples at various predetermined times, the pharmacokinetic profiles of PNOC-PDA/DOX (8 mg/kg DOX equiv.) and free DOX were recorded in **Fig. S9**. As expected, free DOX was rapidly cleared from the plasma whereas $PNOC_{10}$-PDA/DOX and $PNOC_{20}$-PDA/DOX achieved a higher bloodstream DOX concentration and a longer elimination half-life time ($t_{1/2\beta}$) of (4.51 ± 0.6) h and (5.32 ± 0.57) h, which is about

11.0-fold and 13.0-fold compared to (0.41 ± 0.04) h of free DOX, respectively. Moreover, the area under curve (AUC) of $PNOC_{10}$-PDA/DOX and $PNOC_{20}$-PDA/DOX are (117.38 ± 3.67 mg.h/L) and (133.12 ± 4.94 mg.h/L), which is about 32.33-fold and 36.67-fold of (3.63 ± 0.21 mg.h/L) for free DOX, respectively. The polypeptide nanocomposites PNOC-PDA/DOX obviously prolong the blood circulation time of DOX, which is physiologically stable for the following in vivo studies.

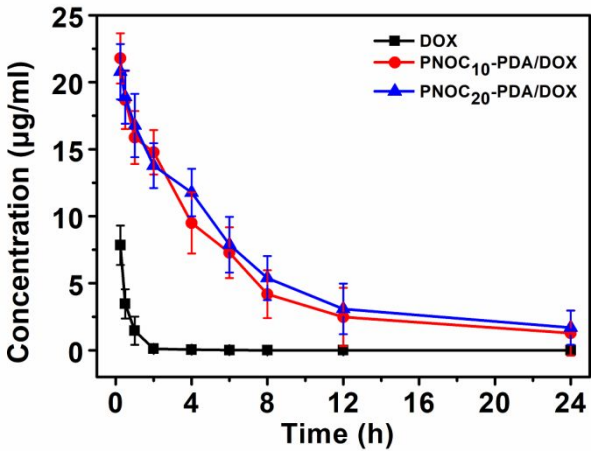

Figure S9. Representative plasma concentration-time profiles of free DOX, $PNOC_{10}$-PDA/DOX and $PNOC_{20}$-PDA/DOX after i.v. injection into rats (a dose of 8 mg/kg). The data are presented as the average ± standard error (n = 4).

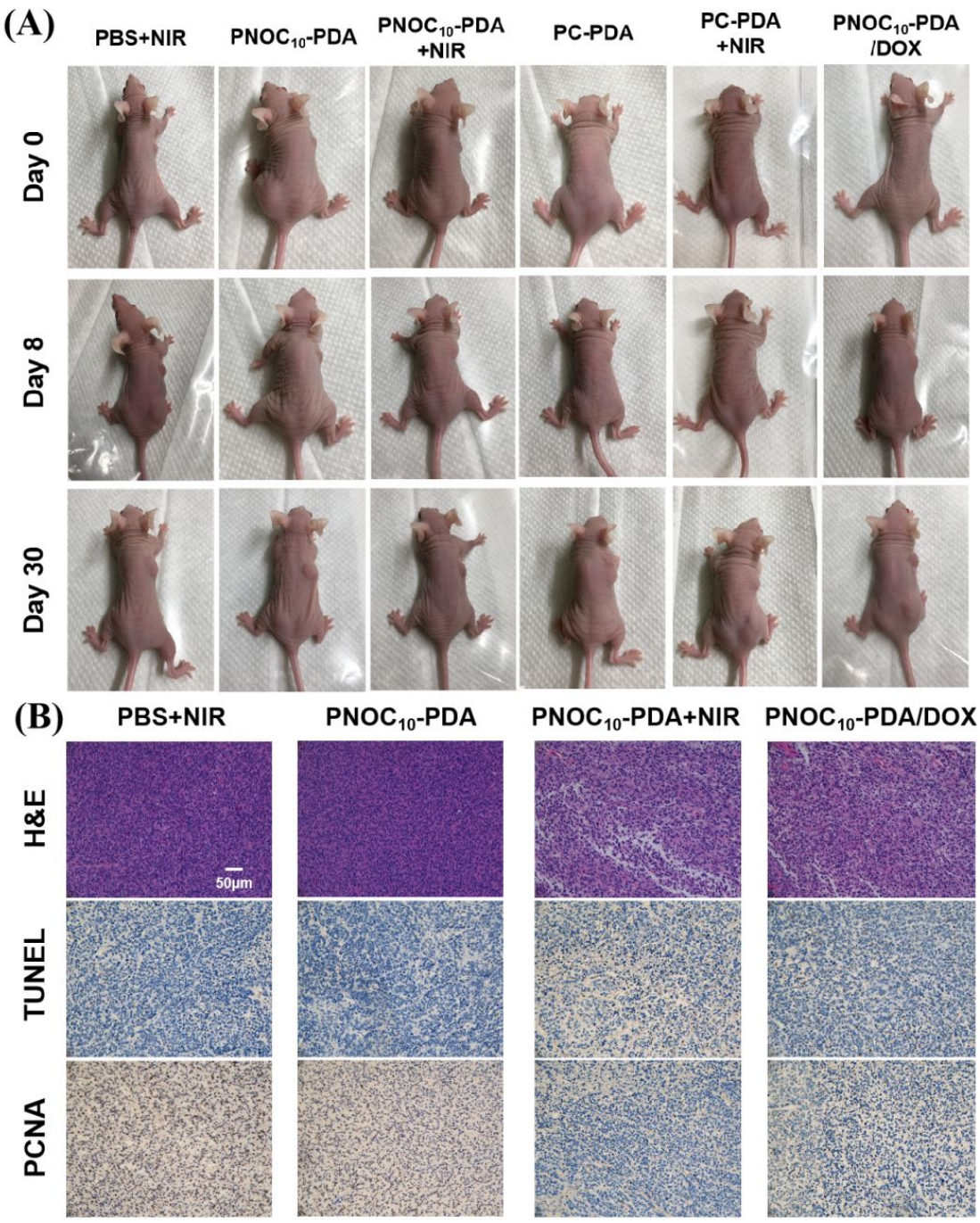

Figure S10. (A) The photographs of the MCF-7/ADR mice with various treatments; (B) H&E, TUNEL, and PCNA assays of the dissected tumors on day 30.

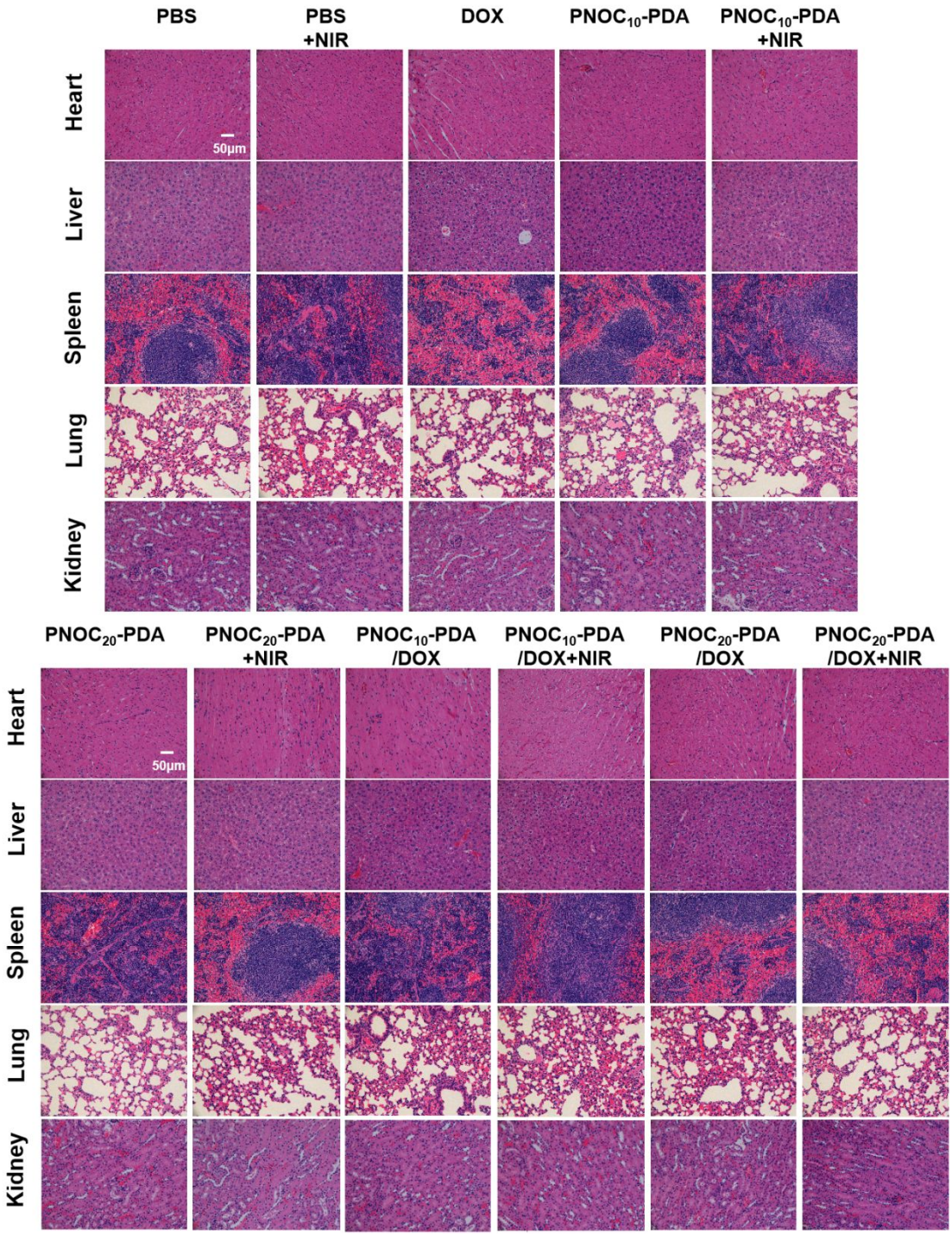

Figure S11. H&E-stained tissue sections from the major organs (heart, liver, spleen, lung, and kidney) dissected on day 30.

References

(1) Liu, G.; Dong, C.-M. *Biomacromolecules* **2012**, *13*, 1573-1583.

(2) Wu, X. J.; Zhou, L.; Su, Y.; Dong, C.-M. *Polym. Chem.* **2015**, *6*, 6857-6869.

(3) Zhang, K.; Xu, H.; Jia, X.; Chen, Y.; Ma, M.; Sun, L.; Chen, H. *ACS Nano* **2016**, *10*, 10816-10828.

(4) Ma, L.; Kohli, M.; Smith, A. *ACS Nano* **2013**, *7*, 9518-9525.